Title: Simulation and techno-economic optimization of the supercritical CO_2 extraction of *Eucalyptus globulus* bark at industrial scale

Authors: Vítor H. Rodrigues, Marcelo M.R. de Melo, Inês Portugal, Carlos M. Silva

PII: S0896-8446(18)30462-5
DOI: https://doi.org/10.1016/j.supflu.2018.11.025
Reference: SUPFLU 4419

To appear in: *J. of Supercritical Fluids*

Received date: 11 July 2018
Revised date: 28 November 2018
Accepted date: 30 November 2018

Please cite this article as: Rodrigues VH, de Melo MMR, Portugal I, Silva CM, Simulation and techno-economic optimization of the supercritical CO_2 extraction of *Eucalyptus globulus* bark at industrial scale, *The Journal of Supercritical Fluids* (2018), https://doi.org/10.1016/j.supflu.2018.11.025

Simulation and techno-economic optimization of the supercritical CO_2 extraction of *Eucalyptus globulus* bark at industrial scale

Vítor H. Rodrigues, Marcelo M.R. de Melo, Inês Portugal, Carlos M. Silva*

Department of Chemistry, CICECO – Aveiro Institute of Materials, University of Aveiro, Campus Universitário de Santiago 3810-193, Aveiro, Portugal

*Corresponding author: carlos.manuel@ua.pt
Department of Chemistry, Associate Laboratory CICECO, University of Aveiro
Campus Universitário de Santiago, 3810-193 Aveiro, PORTUGAL
Tel.: + 351 234 401549; Fax: + 351 234 370084

Graphical abstract

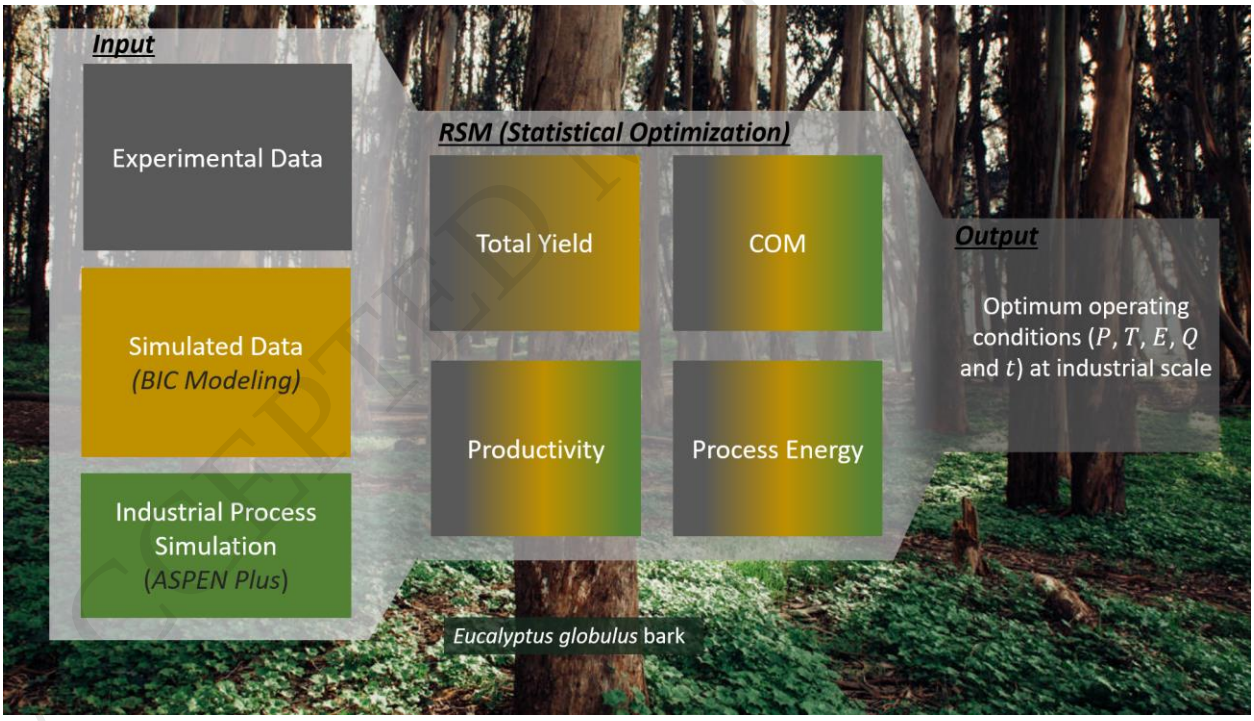

Highlights

- Techno-economic analysis of SFE of *E. globulus* bark at industrial scale.
- Modelling experimental extraction curves and simulation of new ones.
- SFE process design and simulation, including cosolvent recycling.
- Influence of pressure, temperature, ethanol content, CO_2 flow rate and time.
- RSM optimization of Yield, Productivity, Cost of Manufacturing and Process Energy.

ABSTRACT

This work addresses economic and process aspects of the supercritical fluid extraction (SFE) of *Eucalyptus globulus* bark at industrial scale. Broken plus intact cells (BIC) model was applied to existing data and new SFE curves were simulated. Then, statistical optimization was performed with Response Surface Methodology (RSM) involving of 5 factors (pressure, temperature, cosolvent content, solvent flow rate and extraction time), and four responses: Total Yield (η_{Total}), Productivity, Cost of Manufacturing (COM) and Process Energy. The design and simulation of the industrial process (Aspen Plus® software) was performed including the employment of cosolvent in the system. The best COM scored 28.1 $€\ \mathrm{kg}_{\mathrm{extract}}^{-1}$, where η_{Total} was 0.84-0.96 wt.%, Productivity reached 311–362 $\mathrm{ton}_{\mathrm{extract}}\ \mathrm{year}^{-1}$, and Process Energy scored 1.46– 2.10 $\mathrm{GJ}\ \mathrm{kg}_{\mathrm{extract}}^{-1}$. These results underline that SFE provides an extended margin for trade-offs, and arguments towards the integration of SFE technology to biorefine the bark of *E. globulus* in pulp mills.

. List of abbreviations and symbols

a	specific surface area
AARD	average absolute relative deviation
ANOVA	analysis of variance
ATEX	equipment for potentially explosive atmospheres
BIC	broken plus intact cells
BPR	backpressure regulator
CER	constant extraction rate
CRM	raw material cost
COL	cost of operating labor
COM	cost of manufacturing

CUT	utility cost
CWT	waste treatment cost
DC	diffusion controlled
DoE	design of experiments
E	ethanol concentration in the supercritical phase
FCI	investment cost
FER	falling extraction rate
g	grinding efficiency
k_f	external film diffusion coefficient
k_s	intraparticle diffusion coefficient
P	pressure
p (F)	probability of the Fisher distribution
Q	mass flow rate
R^2	coefficient of determination
R^2_{adj}	adjusted coefficient of determination
Re	Reynolds number
RSM	response surface methodology
Sc	Schmidt dimensionless number
SC-CO_2	supercritical carbon dioxide
SFE	supercritical fluid extraction
Sh	Sherwood number
t	time
T	temperature
TTAs	triterpenic acids
u	interstitial velocity
X_0	concentration of the target species in the raw material
X_k	codified value of the independent variable of DoE modeling
Y	DoE response
y^*	solubility
w	mass
w'	mass in a oil free basis
Greek letters	
β	RSM coefficient
ρ	density
ε	porosity

η	yield
Subscript	
annual	relative to a one year period
b	Bed
biomass	relative to the dry biomass
CER	relative to the constant extraction rate period
extract	relative to dry extract
FER	relative to the falling extraction rate period
i	relative to species i
Total	relative to the global extract
0	initial moment
Superscript	
calc	calculated
exp	experimental

Keywords: BIC modeling, Biorefinery, *Eucalyptus globulus* bark, RSM-COM, Supercritical CO_2 extraction.

1. Introduction

Eucalyptus globulus is extensively grown for commercialization in the Mediterranean subtropical regions, specifically in countries like Brazil, China, Portugal, Tasmania, and South Africa. In Portugal, this tree is a key raw material for the pulp and paper industry, and generates significant amounts of byproducts (e.g., bark, leaves, branches, and fruits), typically 4 to 25 ton ha^{-1} [1,2]. Currently, the valorization of such byproducts has been burning for power generation [3,4], which is a low added-value application.

Within the biorefinery scope, *E. globulus* has been object of numerous studies focusing, for example, the valorization of bark through the production of natural extracts by supercritical fluid extraction (SFE) using CO_2 as green solvent [5–10]. The strategy has been the extract enrichment with a class of bioactive compounds known as triterpenic acids (TTAs), which include molecules such as betulinic, betulonic, ursolic, oleanolic acids and the acetylated forms of the last two [11–13]. For *E. globulus* bark, this pathway has been intensively addressed with studies spanning

from: its potential identification [14]; characterization of the morphological parts of the tree (bark, leaves and fruits) [15,16]; preliminary assessment of SFE technology to obtain TTAs [6]; equilibrium and kinetic studies of the extraction [17]; optimization of SFE operating conditions (pressure, temperature, flow rate and cosolvent content) [7,9,18]; study of mass transfer mechanisms and scale-up criterion through experimental SFE curves [9]; and scale-up assays [8].

The Cost of Manufacturing (COM) concept [19] is an useful technique that can anticipate the economic attractiveness of industrial units for the SFE of biomass sources. Its application to SFE has been widely investigated by Meireles, Osorio-Tobón, Santos and Pereira [20–23] and, more recently, by Silva et al. [24]. The latter researchers combined COM and Response Surface Methodology (RSM), giving rise to the RSM-COM approach. This strategy opens the path for lab scale optimization of SFE processes in terms of operating conditions that minimize COM or maximize Productivity at industrial level. The RSM-COM method has been successfully applied to SFE of tomato wastes [24], moringa seeds [25], and gac fruit [26]. In the present work, the RSM-COM methodology will be applied to the SFE of *E. globulus* bark, for which a standard design matrix with experimental data is required. Hence, experimental results were collected from the literature, and phenomenological modeling using the Broken plus Intact Cells (BIC) approach [5,27–29] was applied to the available kinetic curves in order to simulate the missing ones. To the best of our knowledge, it is the first time the whole procedure is implemented.

Globally, the study uses 19 extraction curves, all of them from our research group, which cover the most important SFE operating conditions, namely, pressure, temperature, cosolvent content, solvent flow rate, and extraction time: 8 experimental curves [8,9], 3 final extraction points (for t =6 h), a new experimental curve measured in this work, and 7 purely simulated curves. Simulation of the industrial process was accomplished with Aspen Plus® software. This study intends to offer important techno-economic arguments for the industrial valorization of *E. globulus* bark using supercritical solvent mixtures by a process integration in existing pulp mills. At research level, it enlightens new strategies to overcome lack of experimental data in SFE studies, and it sheds light on the industrial impacts of employing ethanol (the most researched cosolvent [5]) in SFE processes.

2. Modeling

2.1. Modeling of supercritical extraction curves (BIC Model)

The Broken plus Intact Cells (BIC) model was originally proposed by Sovová [27][30] and stands as the most popular comprehensive model within the field of SFE of natural biomass [5]. It considers two distinct domains in ground biomass, namely, intact cells and broken cells. In addition, it assumes that the removal of solutes is driven by convection from broken (external) cells to the supercritical phase, and/or by diffusion from inner intact cells to the outer broken cells.

According to this model, the SFE curves exhibit three distinct regions: a Constant Extraction Rate (CER) period, where the governing resistance is the external film diffusion; a Falling Extraction Rate (FER) period, combining the vanishing convective contribution of CER with the increasingly important intraparticle diffusion from inner intact cells; and a final Diffusion Controlled (DC) period, characterized by a slower rate due to the exclusive dependence on the intraparticle transport. The BIC model calculates the mass of extract (w) produced along time assuming one expression for each period, as follows:

$$w\,(t) = Q\,y^*\,t\,[1-\exp(-Z)] \qquad \text{for } 0 \le t \le t_{\mathrm{CER}} \tag{1}$$

$$w\,(t) = Q\,y^*\,[t - t_{\mathrm{CER}}\exp(Z_m(t) - Z)] \qquad \text{for } t_{\mathrm{CER}} \le t \le t_{\mathrm{FER}} \tag{2}$$

$$w\,(t) = w'_{\mathrm{biomass}}\left\{X_0 - \frac{y^*}{W}\ln\left[1+\left(\exp\left(\frac{WX_0}{y^*}\right)-1\right)\exp\left(\frac{WQ}{w'_{\mathrm{biomass}}}(t_{\mathrm{CER}}-t)\right)\mathrm{g}\right]\right\} \qquad \text{for } t \ge t_{\mathrm{FER}} \tag{3}$$

where Q ($\mathrm{kg\,h^{-1}}$) is the mass flow rate of CO_2, y^* ($\mathrm{kg\,kg^{-1}_{biomass}}$) is the solute (pseudo-component) solubility, t (h) is the extraction time, t_{CER} (h) is the time when the CER period ends, t_{FER} (h) is the time when the FER period finishes, w'_{biomass}(kg) is the mass of dry biomass in solute-free basis, X_0 ($\mathrm{kg\,kg^{-1}}$) is the concentration of extractable target compounds in the raw material, and g is the parameter that represents the fraction of broken cells.

The following expressions complement the three main ones presented above:

$$Z = \frac{k_{\mathrm{f}} a \, w'_{\mathrm{biomass}} \rho_{\mathrm{CO_2}}}{Q \rho_{\mathrm{b}}} \tag{4}$$

$$W = \frac{w'_{\mathrm{biomass}} k_{\mathrm{s}} a}{Q(1-\varepsilon_{\mathrm{b}})} \tag{5}$$

$$t_{\mathrm{CER}} = \frac{(1-g)\, w'_{\mathrm{biomass}}\, X_0}{Q y^* Z} \tag{6}$$

$$t_{\mathrm{FER}} = t_{\mathrm{CER}} + \frac{w'_{\mathrm{biomass}}}{WQ} \ln\left[g + (1-g)\exp\left(\frac{WX_0}{y^*}\right)\right] \tag{7}$$

$$Z_m(t) = \frac{Z y^*}{W\, w'_{\mathrm{biomass}}} \ln\left\{\frac{1}{1-g}\left[\exp\left(\frac{WQ}{w'_{\mathrm{biomass}}}(t - t_{\mathrm{CER}})\right) - g\right]\right\} \tag{8}$$

where ρ_{b} ($\mathrm{kg\,m^{-3}}$) is the bed density, $\rho_{\mathrm{CO_2}}$ ($\mathrm{kg\,m^{-3}}$) is the carbon dioxide density, ε_{b} is the porosity of the bed, k_{f} ($\mathrm{m\,s^{-1}}$) is the convective mass transfer coefficient around broken cells, k_{s} ($\mathrm{m\,s^{-1}}$) is the internal mass transfer coefficient for intact cells, and a ($\mathrm{m^2 m^{-3}}$) is the specific external surface area of the biomass particles.

The total extraction yield is calculated for the whole extract (η_{Total}) by:

$$\eta_{\mathrm{Total}}(\mathrm{wt.\,\%}) = 100 \times \frac{w}{w_{\mathrm{biomass}}} \tag{9}$$

where w_{biomass} (kg) is the mass of dry biomass for each extraction.

The goodness of fit was quantified in this work by the average absolute relative deviation (AARD) defined by:

$$\mathrm{AARD}(\%) = \frac{100}{n}\sum_{i=1}^{n}\left|\frac{\eta_{\mathrm{i}}^{\mathrm{calc}} - \eta_{\mathrm{i}}^{\mathrm{exp}}}{\eta_{\mathrm{i}}^{\mathrm{exp}}}\right| \tag{10}$$

where n is the number of data points of the cumulative extraction curve, and $\eta_{\mathrm{i}}^{\mathrm{calc}}$ and $\eta_{\mathrm{i}}^{\mathrm{exp}}$ are the calculated and experimental extraction yields of point i, respectively.

2.2. Design of Experiments (DoE) and Response Surface Methodology (RSM)

The method consists of a numerical and statistical approach encompassing the fitting of empirical models that ponder the influence of different terms on a response, opening the way to their ranking and to discard the nonsignificant terms. The fitting is usually based on a design of experiments (DoE), to benefit from the maximum information at minimum experimental effort and cost [31]. With these tools, the influence of the factors (independent variables, X_i) on the selected responses (dependent variables, Y) is assessed in terms of linear, non-linear and/or interaction effects.

In this work, a full-factorial DoE comprising five factors with mixed levels (two and three) was planned, resulting in a matrix with 48 points covering all the possible combinations of pressure (P,= 120 – 200 bar), temperature (T = 40 – 60 °C), ethanol content (E = 0 – 5.0 wt.%), SC-CO_2 flow rate (Q = 6 – 12 g min^{-1}) and extraction time (t = 1 – 5 h). These are summarized in Table 1.

The five factors were codified and a second order polynomial with linear, quadratic and binary interactions between factors was fitted to the data:

$$Y = \beta_0 + \sum_{i=1}^{5} \beta_i X_i + \sum_{i=1}^{5} \beta_{ii} X_i^2 + \sum_{i=1}^{5} \sum_{j>i}^{5} \beta_{ij} X_i X_j \quad (11)$$

where β_0 is a constant, β_i, β_{ii} and β_{ij} refer to model coefficients for linear, quadratic and interaction effects, respectively.

Four quantitative responses were investigated in this work: Total Yield (η_{Total}, Eq. 9), COM, Productivity and Process Energy, defined as:

$$\mathrm{COM}\ (€\ \mathrm{kg}_{\mathrm{extract}}^{-1}) = \frac{\mathrm{COM}_{\mathrm{annual}}}{w_{\mathrm{extract,annual}}} \quad (12)$$

$$\text{Productivity } (\text{ton}_{\text{extract}}\ \text{year}^{-1}) = w_{\text{extract,annual}} \quad (13)$$

$$\text{Process Energy } (\text{kJ kg}_{\text{extract}}^{-1}) = \frac{\text{Energy}_{\text{annual}}}{w_{\text{extract,annual}}} \quad (14)$$

where $\text{COM}_{\text{annual}}$ refers to the annual costs of a designed industrial SFE process (presented in Sections 2.3 and 2.4), COM is the cost of manufacturing per mass of extract produced, $w_{\text{extract,annual}}$ is the annual extract mass produced, and $\text{Energy}_{\text{annual}}$ refers to the energy (electricity, steam) consumption for the projected industrial SFE and pretreatment stages during one year of operation.

The statistical analysis was performed using JMP software (version 8.0, SAS Institute Inc., Cary, USA). Analysis of variance (ANOVA) was employed to assess the statistical significance of the effects using Fisher's test and its associated probability $p(F)$, while t-tests were performed to judge the significance of the fitted coefficients of each model. The determination coefficients, R^2, and their adjusted values, R^2_{adj}, were used to evaluate the goodness of the fit of the regression models.

2.3. Design and simulation of the SFE process with ethanol in ASPEN® Plus

Three of the four responses modeled by RSM (i.e. COM, Productivity, and Process Energy) require the capital investment, process costs, and human labor expenses of an industrial SFE unit. Accordingly, a scale-up study based on the lab/modeled results mentioned above is necessary. The utilized scale-up criterion was the flow rate per mass of bark in the extractors, which was previously identified [9] and later confirmed [8] as appropriate.

Taking into account that ethanol can be used a CO_2 modifier in the SFE, two different layouts were considered for simulation: Case A, a scenario without cosolvent, similar to the simplest ones focused in previous works [25,26]; and Case B, a scenario employing ethanol as cosolvent, which includes a new section with additional stages for solvent/cosolvent separation and recirculation. The two layouts are systematized in Table 2 and a full scheme of the processes is provided in

Figure 1, where the upper section refers to Case A, and the grey shaded area comprises the additional flowsheet for cosolvent recovery and recirculation, completing Case B.

The base SFE unit (Case A) encompasses 6 extractors in parallel (represented as XTRACTOR in Fig. 1), each one of 20 m^3 (maximum size implemented at industrial scale [32]), being supported by two modules of equipment, namely, two liquid CO_2 reservoirs (CO2TANK), two CO_2 pumping systems (CO2PUMP), two condensing systems (CO2COND1), two heating systems (HEATER), two BPR valves (FLOWREGU) (plus additional valves) and two extract collection vessels (SEP1). All equipment was sized to satisfy the extractors output. For a fair comparison between the two cases, a compressor (COMP) was exceptionally included in Case A which enables the recovery of the CO_2 lost every time an extractor is opened for biomass reload (otherwise considered a loss and added to the raw material *make-up* costs).

In turn, all of the extra equipment of Case B is owed to process modifications due to the use of the cosolvent. Accordingly, the collection vessels conditions (45 bar and 45 ^oC) were selected from a preliminary analysis of *P*, *T* effect on COM. These vessels stand as flash separators (SEP1) where 98.5 wt.% of the feed CO_2 is recovered in the gas phase (with minor amounts of vaporized ethanol), condensed (CO2COND1) and returned to the CO_2 storage tanks (CO2TANK). The remaining 1.5 wt.% of CO_2 is dissolved in the raffinate liquid stream (containing the dissolved extract) where it represents 26 wt.% of this mixture. This stream is further decompressed (VALV2) to atmospheric pressure and the extract is separated from the solvent mixture by crystallization (a dried powder is obtained) using an evaporator (EVAPORAT), leaving the system through the bottom of the equipment. In turn, the evaporated solvent/cosolvent mixture feeds a flash separator (SEP2) at 1 bar and 0 ^oC (selected to maximize the CO_2/ethanol separation), where ethanol is fully condensed and returned to the ethanol tank (ETHTANK). Finally, the CO_2 stream is compressed (COMP) to 45 bar, condensed (CO2COND1) and returned to the CO_2 tank (CO2TANK).

The simulation of the process was performed using the RK-ASPEN method (based on the Redlich-Kwong-Soave equation of state). To assist the CO_2/ethanol vapor-liquid equilibrium calculations,

thermodynamic data from Mehl et al. [33] were added to ASPEN® *Properties Data* to determine reliable binary parameters by regression.

2.4. Cost of Manufacturing (COM) calculations

The annual COM of a SFE process can be determined by [19]:

$$\mathrm{COM}_{annual} = 0.304\mathrm{FCI} + 2.73\mathrm{COL} + 1.23(\mathrm{CUT} + \mathrm{CWT} + \mathrm{CRM}) \quad (15)$$

where FCI is the fixed cost of investment (with depreciation), COL is the cost of operating labor, CUT is the cost of utilities, CWT is the waste treatment cost, and CRM is the cost of raw materials.

In terms of FCI, the process presented herein can be divided into three sections, as follows:

(i) The SFE plant consists of two SFE sets with 3 extractors in parallel of 20 m^3 each (size selected considering the bark available from a medium-sized pulp and paper mill located in Portugal [34]) according to the specifications of Case A (see Table 2). The price of the SFE plant (excluding the compressor) was estimated according to Lack et al. [35]. The cost of the compressor was estimated using the Module Costing Technique [19]. These values are all reported in Table 3.

(ii) The equipment for case B comprises all the costs of case A plus the purchase of one flash-type separator, one evaporator, one pump and a reservoir for ethanol (see Table 2 and Figure 1), also estimated using the Module Costing Technique [19]. Moreover, since special precautions are needed when using ethanol, such as explosion proof equipment and wiring [36], an ATEX factor (penalty) of two times the cost of a non-hazardous system was adopted.

(iii) Finally, the biomass drying process (common to both cases) is performed in a belt drier to reduce moisture content from *ca*. 35 wt.% to 4 wt.%, using electrical power. The investment costs were determined from the price of a previously reported unit [25], applying a cost factor indexed to the size of the SFE unit.

The full list of assumptions supporting the economic analysis is presented in Table 3. Taking into account this essay refers to a biorefinery to be integrated in an existing pulp mill, the bark is used as produced in the process (particle size of < 2 mm), the storage and transport lines are those available in the facility, as well as all utilities required.

3. Results and discussion

3.1. Database of SFE results

Table 4 reports the complete extraction yield data used in the BIC modeling. These correspond to previous SFE experiments from our research group and thus equal extractor size (0.5 L) and geometry using samples of the same *E. globulus* bark lot ground to a particle size of < 2 mm. In addition it includes lab scale (i.e. 0.5 L) results that were successfully upscaled to 5.0 and 80 L capacity SFE units [8].

Most of the experimental data of Table 4, i.e. Runs 1-8 plus Run 12, were retrieved from previous publications [9][7][8]. They are displayed in two formats: extraction curves (yields along time) and single collection experiments (at fixed extraction time), at different operating conditions, namely, pressure, temperature, cosolvent (ethanol) content, and supercritical CO_2 (SC-CO_2) flow rate. As for Runs 10-11, the yields at $t = 6$ h were estimated using the quadratic yield model previously proposed for the cubic space of operating conditions of 100-200 bar, 40-60 °C, 0-5 wt.% of ethanol (at a constant flow rate of 6 g min^{-1}) [7]. Finally, a new experimental extraction curve (Run 9) was measured in this work following the same procedure of previous studies [7–9]. Accordingly, it took place in a Speed-SFE lab unit from Applied Separations Inc. at 200 bar, 40 °C, 0 wt. % ethanol, 6 g min^{-1} of CO_2, with the extract samples being collected at several times up to 10 h of extraction.

3.2. BIC Modeling results

The experimental data gathered in Table 4 was modeled using the integrated form of BIC model (Eqs. 1-8), in order to determine equilibrium, transport and other important parameters. The results of the modeling work for the 12 experimental SFE curves are presented in Table 5 where it can be noticed that an overall AARD of 7.01 % was obtained. The strategy for the implementation of the BIC model was similar to the one applied for SFE of cork from *Q. cerris* [37], i.e.:

- X_0 assumes different values for assays with different ethanol contents (E);
- $k_f a$ assumes different values for distinct operating conditions (P, T, E or Q);
- $k_s a$ and y^* assume different values for assays with different $P, T,$ or E values;
- g is the same for all assays, as the biomass lot is the same, and particle size remained unchanged in this study;

This approach was particularly useful for the simulation of the new curves, since part of the parameters was immediately fixed.

In cases where the only change is the flow rate (which corresponds to the missing group for the proposed RSM study), the relationship between k_f values of Runs (i and j) can be established from empirical correlations involving Sherwood (Sh), Reynolds (Re) and Schmidt (Sc), like $\mathrm{Sh} = \alpha\,\mathrm{Re}^{\beta}\mathrm{Sc}^{\gamma}$. Accordingly,:

$$\frac{(k_f)_i}{(k_f)_j} = \left(\frac{u_i}{u_j}\right)^{\beta} = \left(\frac{Q_i}{Q_j}\right)^{\beta} \tag{16}$$

where u_i is the fluid velocity, and β scores 0.8 for our experimental conditions (typical for expectable turbulent conditions in the column) [29]. As a result, the $k_f a$ of a new assay can be determined from the coefficient for a different flow rate. This was accomplished for the seven assays at 12 $g_{CO_2}\,\mathrm{min}^{-1}$. (Runs 13 to 19), whose SFE curves were necessary to complete the design matrix of the RSM study; the results achieved are listed in Table 6.

The new simulated curves (Runs 13 to 19) are graphed in Figure 2 together with the curves of Table 5 that are needed for the RSM optimization (Runs 1-6 and 10-12). It can be noticed that the SFE curves exhibit very distinct profiles with a tendency to overlap in the intermediate yield region of 0.4-0.8 wt.%. Four curves at 200 bar with 5 wt.% ethanol stand out as the top

performances. In turn, poor performance is observed for the smoothest conditions, namely 120 bar, 60 °C, 0 wt.% ethanol and 6 g min^{-1} (i.e. Run 10).

3.3. RSM optimization results

The RSM optimization performed in this work intends to maximize the Total Yield (η_{Total}) and Productivity, and to minimize COM and Process Energy of the SFE process. The complete matrix containing the 48 rows of data assays used in the statistical optimization study is presented in Appendix A (Table A1). This matrix was built from experimental data (whenever available), and from the simulated curves discussed in Section 3.1. In such cases, yield values at three extraction times (1, 3 and 5 h) were picked to build the complete matrix. Then, Productivity, COM and Process Energy values corresponding to each row of the matrix (i.e. the reported operating conditions and η_{Total} values) were determined using the methods described in Sections 2.2-2.4.

Once the generic full model (Eq. 11) was fitted to each response, a screening exercise was accomplished to rank and select the significant effects and to discard the nonsignificant ones. Accordingly, Figure 3 presents the Pareto charts for each response, with the global desirable and undesirable effects being represented by blue and orange bars, respectively. The dashed red lines identify the 95 % confidence level limits. The four responses will be analyzed in detail hereafter.

The Pareto charts in Figure 3 show that the Total Yield response has clearly three dominant linear effects: time (t), as the factor that frames the margin for the removal of extractives; pressure (P), due to the higher density and solvent power it imposes to the extraction process; and ethanol content (E) which increases the polarity of the solvent and the solvent power of the supercritical mixture. These three effects have comparable weights, and score almost three times the fourth one, SC-CO_2 flow rate (Q). Finally, the extraction temperature (T) was the least important linear factor and imparts an undesired effect. To comprehend this, one should recall that, for the $P-T$ frame considered, the increase of temperature has conflicting consequences, namely, the increase of solutes vapor pressure and diffusivity (favorable effect), and a decrease of supercritical solvent density (unfavorable effect). In fact, the attained positive importance of P

and E, and the negative contribution of T for η_{Total} have a resemblance with a previous but shorter RSM study (a full factorial of 3 factors and 3 levels) published by Domingues et al. [7].

The Pareto chart for Productivity (Figure 3.C) is very similar to that of Total Yield (Figure 3.A), at least in terms of the importance of P and E factors. These remain the most significant effects, and both contribute in a positive way, maximizing the response. The main difference observed is the significance of the linear effect of extraction time, t, which loses statistical significance in the case of Productivity, falling lower than any of the other linear effects, including of T. In the case of Total Yield, too high extraction times lead to underperformance of the SFE plants due to the lower extraction rates that characterize FER and DC periods. In the case of Productivity, since it corresponds to the cumulative effect of batch extractions over one year, it averages and attenuates the influence of time because the penalizing role of the FER and DC periods is absorbed by the dominant extraction rate of the first period of extraction. On the other hand, both Pareto charts (Figures 3.A and 3.C) present an interesting clear sign that, in the range of operating condition studied, ethanol content and pressure can be deemed alternative and comparable choices to enhance both Total Yield and Productivity responses.

The Pareto chart for COM (Figure 3.B) shows more balanced contributions of the effects. Nevertheless, the linear effect of P is still the most influent, contributing globally to the minimization of this response. This means that an increase of P imposes a simultaneous increase of Total Yield and Productivity, plus a decrease of COM, as desirable. The same behavior is true for E but in a less pronounced way. In fact, the linear effect of E ranks only as the fourth most influent contribution. Such result denotes the modest (but favorable) advantage of operating with ethanol as cosolvent in terms of the COM: the Productivity gains overcome the increased expenses at FCI, CUT and CRM levels and compensate as a process design option.

On the other hand, the second most important factor for COM is T, contributing in the undesired way. This means that it is more cost-effective to run the SFE plant at lower temperatures, which is aligned with the researched trends regarding the typical T chosen for SFE of vegetal biomass [5]. Furthermore, the increase of T necessarily imposes an additional consumption of utilities, which further increases process costs.

Finally, the Process Energy Pareto chart (Figure 3.D) shows a general resemblance with the COM chart. However, a singular difference is found for the linear effect of Q, as the increment of this factor is not able to increase the Productivity (at a given time) enough to compensate the increase of energy consumption for pumping, compressing, heating and cooling (to recover the solvent and cosolvent for reuse). While this clearly penalizes this response, when converted to energy costs, the impact seems to be not relevant for COM due to the dilution of utility expenses with other parcels of the cost structure (recall Eq. (15)).

Optimum operating conditions – After discarding the non-significant effects from the general model (Eq. 11) for each response, the reduced decoded models were produced. These are presented in Table 7, along with the respective coefficients of determination. Accordingly, the models for Total Yield (R^2= 0.919) and Productivity (R^2= 0.868) were the best correlating the experimental data, followed by Process Energy (R^2= 0.771) and then COM (R^2= 0.709). The former two are also the least prone to overfitting, since the R^2_{adj} values are closer to the R^2 , with absolute average deviations of 1.7 % and 2.2 % for Total Yield and Productivity, against 6.1 % for COM and Process Energy models.

The response surface models presented in Table 7 can be plotted to evidence local differences between responses, with special emphasis on the local impact of cumulative effects of linear, non-linear and/or crossed nature. Accordingly, surfaces plots are presented in Figure 4 placing the different responses as function of two factors (Q and t), with the exception of COM, where P replaced Q since the latter is not a significant factor. Comparing the different graphs of Figure 4, it seems that the flow rate should be at its maximum condition value (i.e. 12 $\mathrm{g\,min^{-1}}$), which is in agreement with a previous kinetic study where the external resistance to mass transfer (film) was significantly reduced by increasing the SC-CO_2 flow rate from 6 to 12 $\mathrm{g\,min^{-1}}$, but no apparent gain was found with a further increase to 14 $\mathrm{g\,min^{-1}}$ [9]. As for extraction time, t, the quadratic effect in COM and Productivity shows an optimum region between 2 – 4 h. The optimum conditions for the four studied responses are compiled in Table 8. One can see that the optimum t for COM and Productivity is 3.0 and 2.6 h, respectively. In turn, for η_{Total} and Process Energy the optimum extraction times are 5 and 1 h, respectively. In practice, this means that yield results are not sufficient to choose the preferable t for industrial processes, since process aspects should be considered.

A particularity of the results presented in Table 8 is the coincidence of optimum conditions with extreme values of the experimental design (e.g. maximum pressure, 200 bar, or minimum temperature, 40 ^{o}C).

While, as discussed before, the extraction time can be very different between the responses, a different situation is found for P, T and E, whose optimum values are the

same for η_{Total} ,Productivity , and COM: 200 bar, 40 °C and 5 wt.% of ethanol, respectively (Table 8). The same optimum T and E values also apply to Process Energy, making it very easy to satisfy the best performance in the four responses. In turn, the best conditions for Process Energy, which achieves 0.436 $\mathrm{GJ\ kg_{extract}^{-1}}$, demand P to drop to 120 bar and Q to decrease to 6 $\mathrm{g\ min^{-1}}$.

Globally, the optimum COM scored 28.1 € $\mathrm{kg_{extract}^{-1}}$ at which η_{Total} is 0.84-0.96 wt.%, Productivity reaches 311 – 362 $\mathrm{ton_{extract}\ year^{-1}}$, and Process Energy scores 1.46 – 2.10 $\mathrm{GJ\ kg_{extract}^{-1}}$. These results are very close from those that an optimization based on Productivity would return. However, if optimization would be accomplished based exclusively on η_{Total}, a 43 % higher COM would be achieved, altogether with a lower Productivity (up to 14%). As for the Process Energy, a specific optimization of this response is able to reduce the final score one order of magnitude to 0.436 $\mathrm{GJ\ kg_{extract}^{-1}}$. However, this occurs at the expense of a 67 % higher COM, 60-66 % lower η_{Total}, and 49-56 % lower Productivity (in relation to the optimum conditions reported for COM).

Overall, our results anticipate that bark extracts obtained by SFE are slightly more expensive than the Eucalypt oil [5]. Nevertheless, it should be considered that a typical difficulty, (yet to solve in SFE research), comprises the fair appraisal of the value of natural extracts obtained by green methods, plus the pricing associated to the effectiveness of its biological features.

4. Conclusions

In this work, phenomenological and statistical modeling was performed in order to enable a thorough techno-economic study of SFE of *Eucalyptus globulus* bark. For this, a large set of experimental data was modelled using broken plus intact cells (BIC model) approach and new curves were simulated based on the fitted phenomenological parameters. Moreover, an industrial process was devised and sized (2 sets of 3 extractors of 20 m^3), for which the process simulation Aspen® Plus software was used

to evaluate energy and utilities consumption. Finally, cost of manufacturing (COM) concept was applied to the designed industrial process.

The statistical modeling relied on the response surface methodology (RSM), and comprised data from 16 experimental and predicted extraction curves, in a study of five parameters (pressure, temperature, ethanol content, CO_2 flow rate, and extraction time) and mixed levels (2 and 3). The studied responses were Total Yield (η_{Total}), Productivity, COM and Process Energy.

Taking into account that SFE is a high-pressure technology many times deemed too expensive and energy intensive, the study reinforces the advantage of increasing the pressure to decrease COM, plus to enhance η_{Total} and Productivity. Nevertheless, the optimization results confirm that P enhances the Process Energy of the process.

This work also clarifies the impact of employing a cosolvent in terms of fixed (FCI) and variable costs (CUT, CRM). The best performances in all four responses studied benefit from the presence of ethanol as cosolvent up to 5 wt.%. In contrast, the increase of temperature was shown to be unfavorable to all of the responses, and so the lower temperature (40 °C) is preferable. The best COM scored 28.1 $€\ \mathrm{kg}_{\mathrm{extract}}^{-1}$, where η_{Total} was 0.84-0.96 wt.%, Productivity reached 311 – 362 $\mathrm{ton}_{\mathrm{extract}}\ \mathrm{year}^{-1}$, and Process Energy scored 1.46 – 2.10 $\mathrm{GJ}\ \mathrm{kg}_{\mathrm{extract}}^{-1}$. This result is very close to what an optimization based on Productivity is able to return. In turn, if the optimization would be accomplished based exclusively on η_{Total}, a 43 % higher COM and 14 % lower Productivity would be achieved.

These results underline that SFE provides an extended margin for trade-offs, especially when several factors are allowed to be changed.

In the whole, this study provides techno-economic arguments towards the adoption of SFE technology to valorize the bark of *E. globulus* in a biorefinery context in which the industrial process can be coupled to existing pulp plants handling this vegetal species and currently burning the bark as a residue.

5. Acknowledgments

This work was developed in the scope of: (i) project CICECO-Aveiro Institute of Materials (Ref. FCT UID/CTM/50011/2013), financed by national funds through the FCT/MEC and when applicable co-financed by FEDER under the PT2020 Partnership Agreement; and (ii) Project Inpactus – innovative products and technologies from eucalyptus, Project N.º 21874 funded by Portugal 2020 through European Regional Development Fund (ERDF) in the frame of COMPETE 2020 nº246/AXIS II/2017.

Cofinanciado por:

7. References

[1] I.M. Mirra, T.M. Oliveira, A.M.G. Barros, P.M. Fernandes, Fuel dynamics following fire hazard reduction treatments in blue gum (*Eucalyptus globulus*) plantations in Portugal, For. Ecol. Manage. 398 (2017) 185–195. doi:10.1016/j.foreco.2017.05.016.

[2] P.M. Fernandes, C. Loureiro, P. Palheiro, H. Vale-Gonçalves, M.M. Fernandes, M.G. Cruz, Fuels and Fire Hazard in blue gum (*Eucalyptus globulus*) stands in Portugal, Boletín Del CIDEU. 10 (2011) 53–61.

[3] S. Pérez, C.J. Renedo, A. Ortiz, M. Mañana, D. Silió, Energy evaluation of the *Eucalyptus globulus* and the *Eucalyptus nitens* in the north of Spain (Cantabria), Thermochim. Acta. 451 (2006) 57–64. doi:10.1016/j.tca.2006.08.009.

[4] L. Núnez-Regueira, J. Proupín-Castieiras, J.A. Rodríguez-Aón, Energy evaluation of forest residues originated from *Eucalyptus globulus* Labill in Galicia, Bioresour. Technol. 82 (2002) 5–13. doi:10.1016/S0960-8524(01)00156-0.

[5] M.M.R. De Melo, A.J.D. Silvestre, C.M. Silva, Supercritical fluid extraction of vegetable matrices: Applications, trends and future perspectives of a convincing green technology, J. Supercrit. Fluids. 92 (2014) 115–176. doi:10.1016/j.supflu.2014.04.007.

[6] R.M.A. Domingues, E.L.G. Oliveira, C.S.R. Freire, R.M. Couto, P.C. Simões, C.P. Neto, A.J.D. Silvestre, C.M. Silva, Supercritical fluid extraction of *Eucalyptus globulus* bark-A promising approach for triterpenoid production, Int. J. Mol. Sci. 13 (2012) 7648–7662. doi:10.3390/ijms13067648.

[7] R.M.A. Domingues, M.M.R. De Melo, E.L.G. Oliveira, C.P. Neto, A.J.D. Silvestre, C.M. Silva, Optimization of the supercritical fluid extraction of triterpenic acids from *Eucalyptus globulus* bark using experimental design, J. Supercrit. Fluids. 74 (2013) 105–114. doi:10.1016/j.supflu.2012.12.005.

[8] M.M.R. de Melo, R.M.A. Domingues, M. Sova, E. Lack, H. Seidlitz, F. Lang Jr., A.J.D. Silvestre, C.M. Silva, Scale-up studies of the supercritical fluid extraction of triterpenic acids from *Eucalyptus globulus* bark, J. Supercrit. Fluids. 95 (2014) 44–50. doi:10.1016/j.supflu.2014.07.030.

[9] R.M.A. Domingues, M.M.R. De Melo, C.P. Neto, A.J.D. Silvestre, C.M. Silva, Measurement and modeling of supercritical fluid extraction curves of *Eucalyptus globulus* bark: Influence of the operating conditions upon yields and extract composition, J. Supercrit. Fluids. 72 (2012) 176–185. doi:10.1016/j.supflu.2012.08.010.

[10] S.A.O. Santos, J.J. Villaverde, C.M. Silva, C.P. Neto, A.J.D. Silvestre, Supercritical fluid extraction of phenolic compounds from Eucalyptus globulus Labill bark, J. Supercrit. Fluids. 71 (2012) 71–79. doi:10.1016/j.supflu.2012.07.004.

[11] L. López-Hortas, P. Pérez-Larrán, M.J. González-Muñoz, E. Falqué, H. Domínguez, Recent developments on the extraction and application of ursolic acid. A review, Food Res. Int. 103 (2018) 130–149. doi:10.1016/j.foodres.2017.10.028.

[12] M. Kvasnica, M. Urban, N.J. Dickinson, J. Sarek, Pentacyclic triterpenoids with nitrogen- and sulfur-containing heterocycles: synthesis and medicinal significance, Nat. Prod. Rep. 32 (2015) 1303–1330. doi:10.1039/C5NP00015G.

[13] R. Domingues, A. Guerra, M. Duarte, C. Freire, C. Neto, C. Silva, A. Silvestre, Bioactive Triterpenic Acids: From Agroforestry Biomass Residues to Promising Therapeutic Tools, Mini. Rev. Org. Chem. 11 (2014) 382–399. doi:10.2174/1570193X113106660001.

[14] C.S.R. Freire, A.J.D. Silvestre, C.P. Neto, J.A.S. Cavaleiro, Lipophilic Extractives of the Inner and Outer Barks of *Eucalyptus globulus*, Holzforschung. 56 (2002) 372–379. doi:10.1515/HF.2002.059.

[15] R.M.A. Domingues, G.D.A. Sousa, C.S.R. Freire, A.J.D. Silvestre, C.P. Neto, *Eucalyptus globulus* biomass residues from pulping industry as a source of high value triterpenic compounds, Ind. Crops Prod. 31 (2010) 65–70. doi:10.1016/j.indcrop.2009.09.002.

[16] V.H. Rodrigues, M.M.R. de Melo, I. Portugal, C.M. Silva, Extraction of *Eucalyptus* leaves using solvents of distinct polarity. Cluster analysis and extracts characterization, J. Supercrit. Fluids. 135 (2018) 263–274. doi:10.1016/j.supflu.2018.01.010.

[17] M.M.R. de Melo, E.L.G. Oliveira, A.J.D. Silvestre, C.M. Silva, Supercritical fluid extraction of triterpenic acids from *Eucalyptus globulus* bark, J. Supercrit. Fluids. 70 (2012) 137–145. doi:http://dx.doi.org/10.1016/j.supflu.2012.06.017.

[18] V.H. Rodrigues, M.M.R. de Melo, I. Portugal, C.M. Silva, Supercritical fluid extraction of *Eucalyptus globulus* leaves. Experimental and modelling studies of the influence of operating conditions and biomass pretreatment upon yields and kinetics, Sep. Purif. Technol. 191 (2018) 173–181. doi:10.1016/j.seppur.2017.09.026.

[19] R. Turton, R.C. Bailie, W.B. Whiting, J.A. Shaeiwitz, D. Bhattacharyya, Analysis , Synthesis , and Design of Chemical Processes, 4th ed., Prentice Hall, 2012. https://books.google.com.br/books?id=f6sbYJuFSycC.

[20] M.A.A. Meireles, Supercritical extraction from solid: Process design data (2001-2003), Curr. Opin. Solid State Mater. Sci. 7 (2003) 321–330. doi:10.1016/j.cossms.2003.10.008.

[21] J.F. Osorio-Tobón, P.I.N. Carvalho, M.A. Rostagno, A.J. Petenate, M.A.A. Meireles, Extraction of curcuminoids from deflavored turmeric (*Curcuma longa* L.) using pressurized liquids: Process integration and economic evaluation, J. Supercrit. Fluids. 95 (2014) 167–174. doi:10.1016/j.supflu.2014.08.012.

[22] D.T. Santos, P.C. Veggi, M.A.A. Meireles, Optimization and economic evaluation of pressurized liquid extraction of phenolic compounds from jabuticaba skins, J. Food Eng. 108 (2012) 444–452. doi:10.1016/j.jfoodeng.2011.08.022.

[23] C.G. Pereira, M.A.A. Meireles, Supercritical fluid extraction of bioactive compounds: Fundamentals, applications and economic perspectives, Food Bioprocess Technol. 3 (2010) 340–372. doi:10.1007/s11947-009-0263-2.

[24] A.F. Silva, M.M.R. de Melo, C.M. Silva, Supercritical solvent selection (CO2 versus ethane) and optimization of operating conditions of the extraction of lycopene from tomato residues: Innovative analysis of extraction curves by a response surface methodology and cost of manufacturing hybrid ap, J. Supercrit. Fluids. 95 (2014) 618–627. doi:10.1016/j.supflu.2014.09.016.

[25] P.F. Martins, M.M.R. de Melo, C.M. Silva, Techno-economic optimization of the subcritical fluid extraction of oil from *Moringa oleifera* seeds and subsequent production of a purified sterols fraction, J. Supercrit. Fluids. 107 (2016) 682–689. doi:10.1016/j.supflu.2015.07.031.

[26] P.F. Martins, M.M.R. de Melo, C.M. Silva, Gac oil and carotenes production using supercritical CO_2: Sensitivity analysis and process optimization through a RSM–COM hybrid approach, J. Supercrit. Fluids. 100 (2015) 97–104. doi:10.1016/j.supflu.2015.02.023.

[27] H. Sovová, Rate of the vegetable oil extraction with supercritical CO_2—I. Modelling of extraction curves, Chem. Eng. Sci. 49 (1994) 409–414. doi:10.1016/0009-2509(94)87012-8.

[28] H. Sovová, Broken-and-intact cell model for supercritical fluid extraction: Its origin and limits, J. Supercrit. Fluids. 129 (2017) 3–8. doi:10.1016/j.supflu.2017.02.014.

[29] E.L.G. Oliveira, A.J.D. Silvestre, C.M. Silva, Review of kinetic models for supercritical fluid extraction, Chem. Eng. Res. Des. 89 (2011) 1104–1117. doi:10.1016/j.cherd.2010.10.025.

[30] H. Sovová, Mathematical model for supercritical fluid extraction of natural products and extraction curve evaluation, J. Supercrit. Fluids. 33 (2005) 35–52. doi:10.1016/j.supflu.2004.03.005.

[31] M.A. Bezerra, R.E. Santelli, E.P. Oliveira, L.S. Villar, L.A. Escaleira, Response surface methodology (RSM) as a tool for optimization in analytical chemistry, Talanta. 76 (2008) 965–977. doi:10.1016/j.talanta.2008.05.019.

[32] NATEX, Project References - NATEX Prozesstechnologie GesmbH, (2018).

https://www.natex.at/about-us/project-references/ (accessed January 10, 2017).

[33] A. Mehl, F.P. Nascimento, P.W. Falcão, F.L.P. Pessoa, L. Cardozo-Filho, Vapor-Liquid Equilibrium of Carbon Dioxide + Ethanol: Experimental Measurements with Acoustic Method and Thermodynamic Modeling, J. Thermodyn. 2011 (2011) 1–11. doi:10.1155/2011/251075.

[34] The Navigator Company, Relatório e contas 2015, 2016. http://www.thenavigatorcompany.com/Investidores/Informacao-Financeira.

[35] E. Lack, T. Gamse, R. Marr, Separation operations and equipment, in: A. Bertucco, G. Vetter (Eds.), High Press. Technol. Fundam. Appl., 1st ed., Elsevier, Amsterdam, 2001.

[36] K.L. Mulholland, J.A. Dyer, Pollution Prevention:Methodology, Technologies and Practices, 1st ed., American Institute of Chemical Engineers, New York, 2015.

[37] M.M.R. De Melo, A. Şen, A.J.D. Silvestre, H. Pereira, M. Carlos, Experimental and modeling study of supercritical CO_2 extraction of *Quercus cerris* cork : influence of ethanol and particle size on extraction kinetics and selectivity to friedelin, Sep. Purif. Technol. (2017). doi:10.1016/j.seppur.2017.06.011.

Appendix A

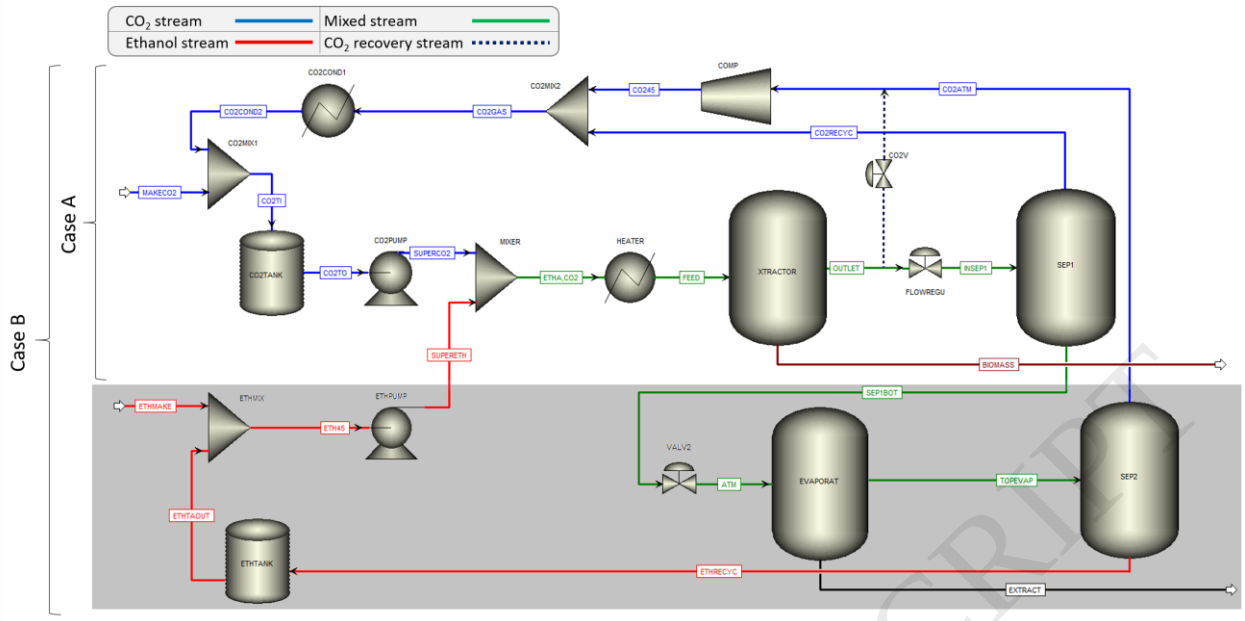

Figure 1 – Flowsheet of the process simulated in ASPEN® Plus software for Case B (employing ethanol as cosolvent), with the respective legend. Case A corresponds to the white area, which does not employ cosolvent. The CO_2 recovery stream (dashed) was added to the flowsheet to stress its inclusion in the process. For simplicity the 6 extractors considered are lumped in the XTRACTOR box.

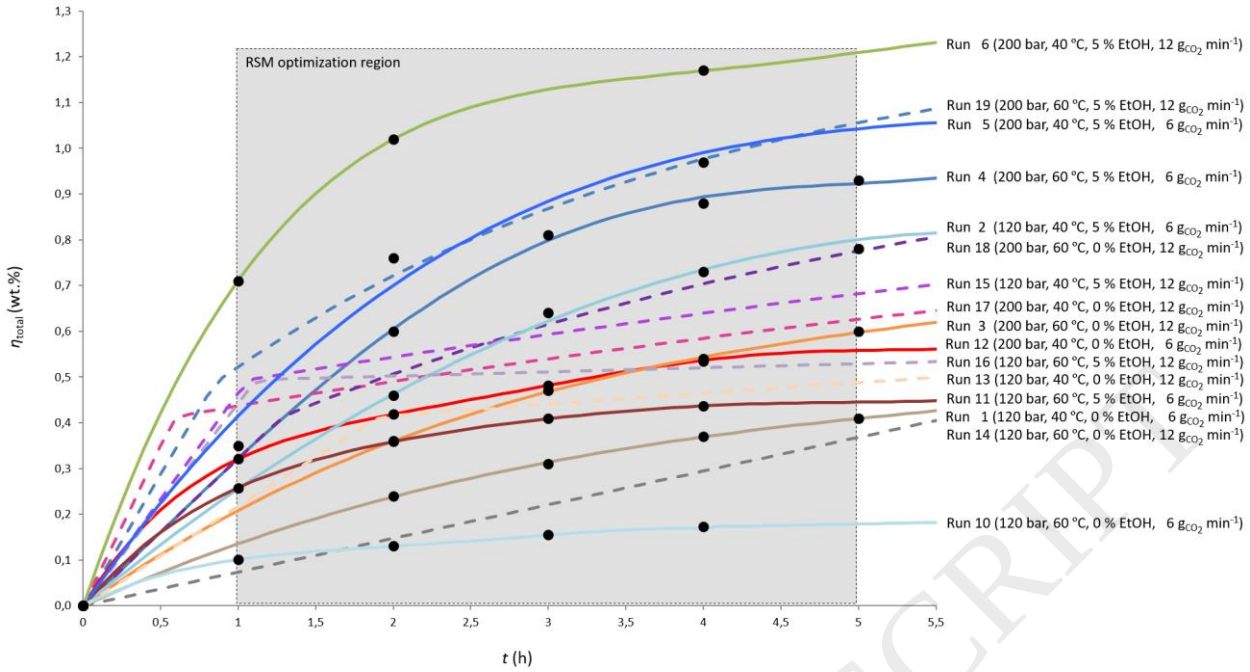

Figure 2 – SFE curves (experimental and simulated) generated using BIC model for the runs needed for the RSM optimization. Dots are experimental data, full lines represent modeling of experimental assays, and dashed lines are purely simulated curves.

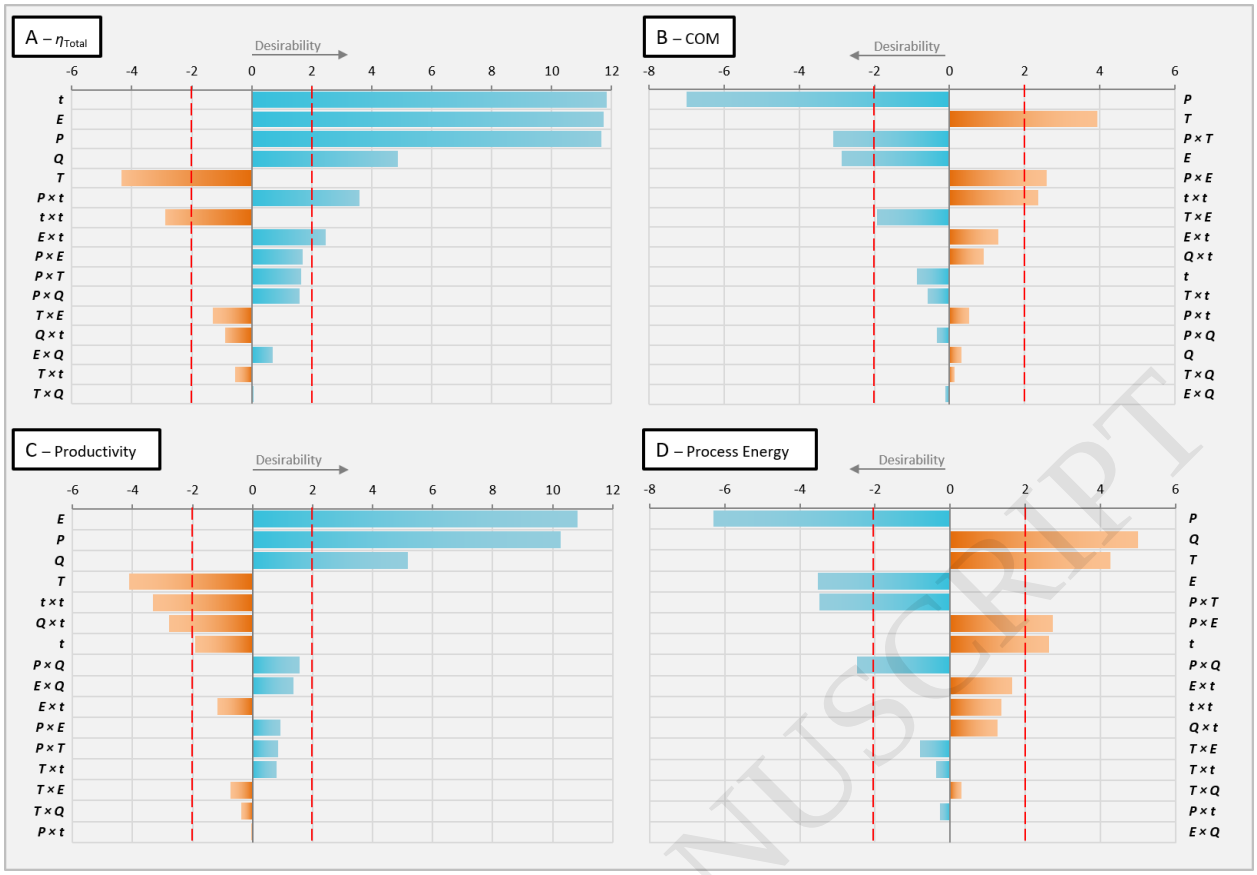

Figure 3 – Pareto charts obtained for each response, with the blue and orange lines representing desired and undesired effects, respectively. The dashed red line corresponds to the significance level for a 95 % confidence level.

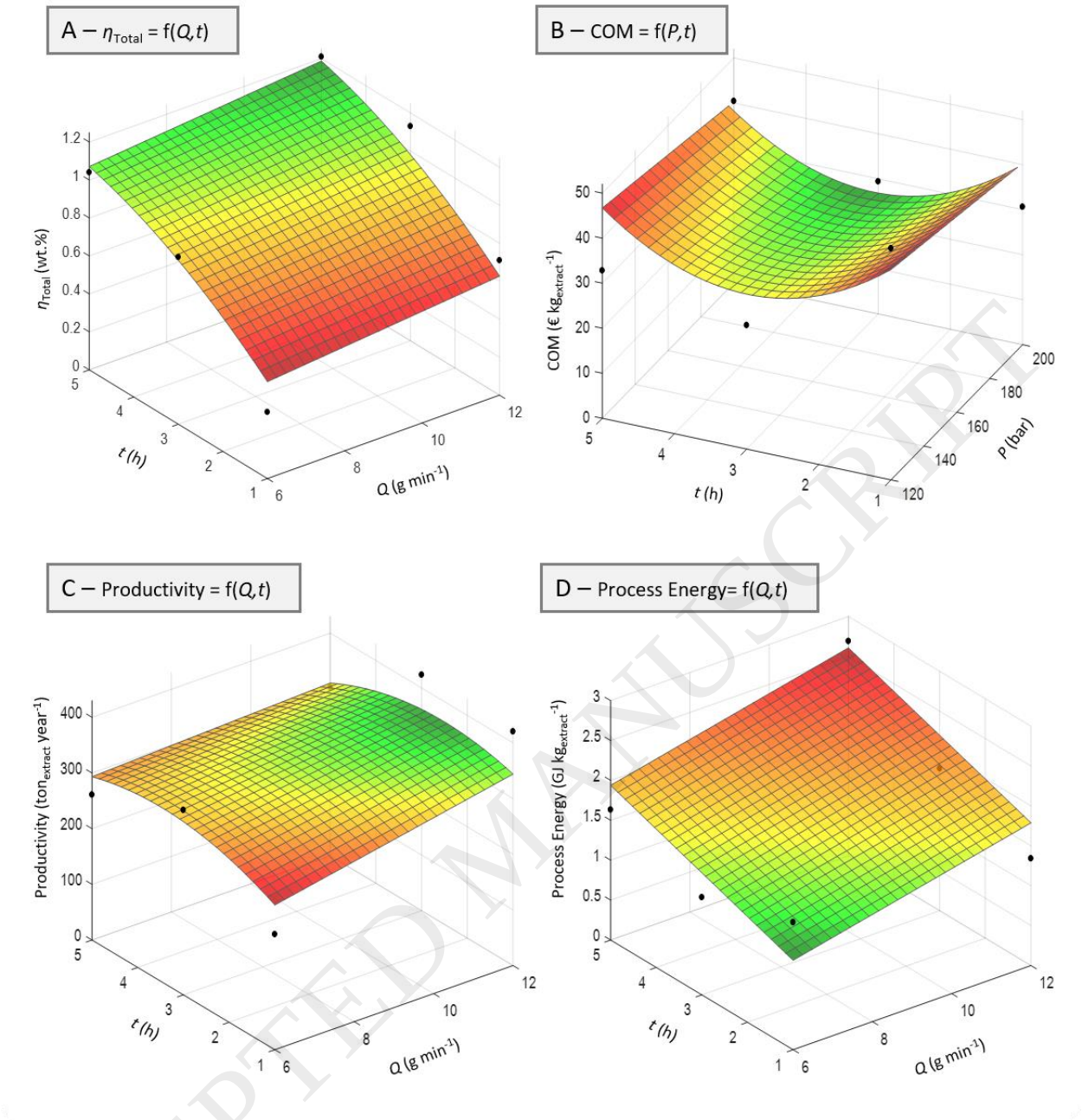

Figure 4 – Response surfaces obtained for Total Yield, COM, Productivity and Process Energy as function of Q and t (P instead of Q for COM) as factors, while P, T and E are fixed at 200 bar, 40 °C and 5.0 wt.% ethanol, respectively.

Table 1 – Correspondence between levels of the five factors in the codified and non-codified form.

Variable	Level correspondence		
	Low (-1)	Medium (0)	High (+1)
Pressure (P, bar)	120	-	200
Temperature (T, °C)	40	-	60
Ethanol content (E, wt.%)	0	-	5
SC-CO_2 flow rate (Q, $\mathrm{g\ min^{-1}}$)	6	-	12
time (t, h)	1	3	5

Table 2 – Equipment of the SFE units using pure CO_2 (Case A) and CO_2 modified with ethanol (Case B).

Equipment		Case A (Pure CO_2)	Case B (CO_2 with ethanol)
Pretreatment	Belt dryer	✓	✓
SFE unit	Extractors	✓	✓
	CO_2 storage tanks	✓	✓
	Pumps	✓	✓
	Heaters	✓	✓
	Condensers	✓	✓
	Sets of valves	✓	✓
	Collection vessels/ Separators	✓	✓
CO_2 recovery	Compressor	✓	✓
Ethanol related equipment	Ethanol storage tank	-	✓
	Pump	-	✓
	Evaporator	-	✓
	Separator	-	✓

Table 3 – List of assumptions considered for the application of COM methodology.

General		- Unit working period: 24 h per day; 330 days per year
		- No. of workers per extractor: 1
		- Scale-up criteria: solvent flow rate per mass of dry bark ($Q\ w_{\mathrm{biomass}}^{-1}$)
		- Required time to unload, load and pressurize extractor (t_{prep}): 1 h
		- Minimum pressure in the extract collection vessel: 45 bar
		- The fluid losses in each full decompression at the end of each cycle are the mass of ethanol inside the extractor at 45 bar and 40 °C
		- Bed porosity: 0.78 [9]
		- Exchange rate (January 2017): 0.931923 € $\mathrm{\$US^{-1}}$
		- Biomass initial moisture: Winter – 50 wt.%; Summer – 20 wt.% - CO_2 recovery: 100 %
		- CO_2 renewal: 5 % of the CO_2 recovered in each full decompression at 45 bar and 40 °C (end of each cycle)
		- Dried wood heat capacity: 0.912 $\mathrm{kJ\ kg^{-1}\ K^{-1}}$ [37]
		- Bark availability: 59.2 $\mathrm{kton\ year^{-1}}$
FCI		- Annual depreciation rate: 10 %
	Case A	- Price of drying unit: 1.44 M€
		- Price of SFE unit, 2 sets of 3 extractors (20 m^3 each): 12.5 M€
		- Price of compressor: 2.30 M€
	Case B	- ATEX factor: 2
		- Price of drying unit: 2.88 M€
		- Price of SFE unit, 2 sets of 3 extractors (20 m^3 each): 25.0 M€
		- Price of ethanol associated equipment and compressor: 15.6 M€
COL		- Labor cost: 10 $\mathrm{€\ h^{-1}\ worker^{-1}}$
CUT		- Cost of electricity: 46.60 $\mathrm{€\ MWh^{-1}}$
		- Cost of steam: 1.86 $\mathrm{€\ ton^{-1}}$
CWT		- Cost of waste treatment: 0 €
CRM		- Cost of bark drying (winter and summer): 0.012 $\mathrm{€\ kg_{bark}^{-1}}$ - Cost of ethanol: 1000 $\mathrm{€\ ton^{-1}}$
		- Cost of CO_2: 800 $\mathrm{€\ ton^{-1}}$

Table 4 – Total yield (wt.%) of the supercritical fluid extraction of *E. globulus* bark. Experimental data taken from literature for the same extractor (0.5 L), biomass lot, and particle size (< 2 mm).

#	P (bar)	T (°C)	E (wt.%)	Q (g min^{-1})	t (h)												Ref
					0.5	1	1.5	2	3	4	4.5	5	6	6.5	8	10	
1	120	40	0.0	6	-	-	-	0.24	0.31	0.37	-	0.41	0.44	-	-	-	[9]
2	120	40	5.0	6	-	-	-	0.46	0.64	0.73	-	0.78	0.83	-	-	-	[9]
3	200	60	0.0	6	-	-	-	0.36	0.47	0.54	-	0.60	0.64	-	-	-	[9]
4	200	60	5.0	6	-	-	-	0.6	0.81	0.88	-	0.93	0.96	-	-	-	[9]
5	200	40	5.0	6	-	0.35	-	0.76	-	0.97	-	-	1.07	-	-	1.18	[9]
6	200	40	5.0	12	-	0.71	-	1.02	-	1.17	-	-	1.25	-	-	1.33	[9]
7	200	40	5.0	14	-	0.72	-	0.98	-	1.14	-	-	1.23	-	-	1.32	[9]
8	200	40	2.5	12	0.36	0.63	0.79	0.88	-	-	0.98	-	-	1.05	-	-	[8]
9	200	60	0.0	8	-	0.42	-	0.58	0.66	0.74	-	-	0.85	-	0.92	0.97	This work
10	120	60	0.0	6	-	-	-	-	-	-	-	-	0.19	-	-	-	[7]
11	120	60	5.0	6	-	-	-	-	-	-	-	-	0.48	-	-	-	[7]
12	200	40	0.0	6	-	-	-	-	-	-	-	-	0.57	-	-	-	[7]

Table 5 – BIC model results obtained for the experimental database of total extraction yield (η_{Total}) compiled in Table 4.

Curve	P (bar)	T (°C)	E (wt.%)	Q (g min^{-1})	model parameters					AARD (%)
					$k_{\mathrm{f}}a$ (h^{-1})	$k_{\mathrm{s}}a$ (10^{-2} h^{-1})	y^*	g	X_0 (kg kg^{-1})	
Run 1	120	40	0.0	6	0.103	0.86	0.0028	0.68	0.0108	4.52
Run 2	120	40	5.0	6	0.030	4.07	0.0176		0.0127	3.36
Run 3	200	60	0.0	6	0.096	4.78	0.0044		0.0108	10.53
Run 4	200	60	5.0	6	0.128	7.08	0.0059		0.0127	5.68
Run 5	200	40	5.0	6	0.058	13.01	0.0133		0.0127	10.44
Run 6	200	40	5.0	12	0.141	13.01	0.0133		0.0127	4.12
Run 7	200	40	5.0	14	0.147	13.01	0.0133		0.0127	3.70
Run 8	200	40	2.5	12	0.277	25.53	0.0057		0.0099	1.75
Run 9	200	60	0.0	8	0.307	4.78	0.0044		0.0108	2.77
Run 10	120	60	0.0	6	0.113	0.30	0.0014		0.0108	36.78
Run 11	120	60	5.0	6	0.034	0.26	0.0191		0.0127	2.17
Run 12	200	40	0.0	6	0.143	1.96	0.0057		0.0108	5.9
Total										7.01

Table 6 – BIC model parameters for the simulated total extraction yield (η_{Total}) curves needed to complete the design matrix of the RSM study.

Curve	P (bar)	T (°C)	E (wt.%)	Q ($\mathrm{g\ min^{-1}}$)	$k_{\mathrm{f}}a$ ($\mathrm{h^{-1}}$)	$k_{\mathrm{s}}a$ ($10^{-2}\ \mathrm{h^{-1}}$)	y^*	g	X_0 ($\mathrm{kg\ kg^{-1}}$)
Run 13	120	40	0	12	0.179	0.86	0.00288	0.68	0.0108
Run 14	120	60	0	12	0.197	0.30	0.0014		0.0108
Run 15	120	40	5	12	0.053	1.54	0.0180		0.0127
Run 16	120	60	5	12	0.060	0.26	0.0191		0.0127
Run 17	200	40	0	12	0.248	1.96	0.0057		0.0108
Run 18	200	60	0	12	0.167	4.78	0.0044		0.0108
Run 19	200	60	5	12	0.223	7.08	0.0059		0.0127

Table 7 – Effects coefficients of the reduced model of each response and respective coefficient and adjusted coefficient of determination.

Coefficient	Effect	η_{Total} (wt.%)	COM ($€\ \mathrm{kg}_{\mathrm{extract}}^{-1}$)	Productivity ($\mathrm{ton}_{\mathrm{extract}}\ \mathrm{year}^{-1}$)	Process Energy ($\mathrm{GJ\ kg}_{\mathrm{extract}}^{-1}$)
β_0	-	-0.1016	-23.51	-168.74	-10.034
β_1	P	0.0015	0.36	1.26	0.050
β_2	T	-0.0052	4.01	-2.02	0.231
β_3	E	0.0344	-13.01	21.18	-0.736
β_4	Q	0.0194	-	16.79	0.631
β_5	t	0.0734	-18.44	76.79	0.205
β_{12}	$P \times T$	-	-0.02	-	-1.10×10^{-3}
β_{13}	$P \times E$	-	0.06	-	3.48×10^{-3}
β_{14}	$P \times Q$	-	-	-	-2.62×10^{-3}
β_{15}	$P \times t$	0.0007	-	-	-
β_{35}	$E \times t$	0.0073	-	-	-
β_{45}	$Q \times t$	-	-	-2.78	-
β_{55}	$t \times t$	-0.0183	3.07	-8.62	-
R^2		0.919	0.709	0.868	0.771
R^2_{adj}		0.903	0.666	0.849	0.724

Table 8 – Optimum conditions for each response and their values under these conditions.

		η_{Total} (wt.%)	COM (€ $\mathrm{kg}_{\mathrm{extract}}^{-1}$)	Productivity ($\mathrm{ton}_{\mathrm{extract}}$ year^{-1})	Process Energy (GJ $\mathrm{kg}_{\mathrm{extract}}^{-1}$)
Optimum Conditions	P (bar)	200	200	200	120
	T (°C)	40	40	40	40
	E (wt. %)	5	5	5	5
	Q (g min^{-1})	12	6-12	12	6
	t (h)	5.0	3.0	2.6	1.0
η_{Total} (wt.%)		1.15	0.84 - 0.96	0.90	0.33
COM (€ $\mathrm{kg}_{\mathrm{extract}}^{-1}$)		40.4	28.1	28.7	46.8
Productivity ($\mathrm{ton}_{\mathrm{extract}}$ year^{-1})		310	311 – 362	364	159
Process Energy (GJ $\mathrm{kg}_{\mathrm{extract}}^{-1}$)		2.51	1.46 – 2.10	2.01	0.436

Table A1 – Complete set of decoded values of variables and responses for the DoE matrix employed in this study.

Run	P (bar)	T (°C)	E (wt.%)	Q (g min^{-1})	t (h)	η_{Total} (wt.%)	COM (€ $\mathrm{kg}_{\mathrm{extract}}^{-1}$)	Productivity ($\mathrm{ton}_{\mathrm{extract}}$ year^{-1})	Process Energy (GJ $\mathrm{kg}_{\mathrm{extract}}^{-1}$)
1	120	40	0	6	1	0.14	81.21	80	3.02
2	120	40	0	6	3	0.31	49.4	116	2.39
3	120	40	0	6	5	0.41	52.9	103	2.78
4	120	40	5	6	1	0.25	69.2	151	0.96
5	120	40	5	6	3	0.64	37.1	240	0.55
6	120	40	5	6	5	0.78	42.6	195	0.63
7	120	60	0	6	1	0.10	108.5	60	3.48
8	120	60	0	6	3	0.16	98.4	58	3.89
9	120	60	0	6	5	0.18	121.2	45	5.11
10	120	60	5	6	1	0.26	68.3	153	2.20
11	120	60	5	6	3	0.41	57.9	154	2.66
12	120	60	5	6	5	0.44	74.6	111	3.84
13	200	40	0	6	1	0.32	35.3	190	1.27
14	200	40	0	6	3	0.48	33.1	181	1.54
15	200	40	0	6	5	0.56	40.4	140	2.04
16	200	40	5	6	1	0.35	51.4	207	1.60
17	200	40	5	6	3	0.88	27.5	332	1.22
18	200	40	5	6	5	1.04	32.8	261	1.63
19	200	60	0	6	1	0.21	54.4	123	2.05
20	200	60	0	6	3	0.47	33.8	176	1.60
21	200	60	0	6	5	0.60	37.6	150	1.92
22	200	60	5	6	1	0.32	56.0	190	1.79
23	200	60	5	6	3	0.81	30.0	304	1.35
24	200	60	5	6	5	0.93	36.7	233	1.84
25	120	40	0	12	1	0.22	61.2	128	3.09
26	120	40	0	12	3	0.44	47.0	165	3.05
27	120	40	0	12	5	0.49	62.9	122	4.39
28	120	40	5	12	1	0.46	45.8	275	2.07
29	120	40	5	12	3	0.59	54.3	223	3.40
30	120	40	5	12	5	0.68	69.4	171	4.77
31	120	60	0	12	1	0.07	180.9	44	9.29
32	120	60	0	12	3	0.22	94.1	83	6.14
33	120	60	0	12	5	0.37	83.5	92	5.85
34	120	60	5	12	1	0.44	48.0	261	2.18
35	120	60	5	12	3	0.51	62.9	192	3.95
36	120	60	5	12	5	0.53	89.3	132	6.16

37	200	40	0	12	1	0.44	31.5	259	1.51
38	200	40	0	12	3	0.54	40.1	203	2.48
39	200	40	0	12	5	0.63	51.3	157	3.41
40	200	40	5	12	1	0.71	30.6	420	1.34
41	200	40	5	12	3	1.13	29.4	424	1.78
42	200	40	5	12	5	1.21	40.4	303	2.69
43	200	60	0	12	1	0.32	42.8	190	2.12
44	200	60	0	12	3	0.62	35.2	231	2.20
45	200	60	0	12	5	0.78	41.4	194	2.77
46	200	60	5	12	1	0.52	41.6	309	1.86
47	200	60	5	12	3	0.87	38.1	326	2.33
48	200	60	5	12	5	1.06	46.3	264	3.09